

Investigation of Microstructure, Heat Treatment and Hydroxyapatite Addition in Selective Laser Melting of Ti6Al4V Alloys

Dissertation Booklet

For the degree of Doctor of Philosophy in Materials Science and Engineering award at the
Doctoral School of Materials Science and Technologies

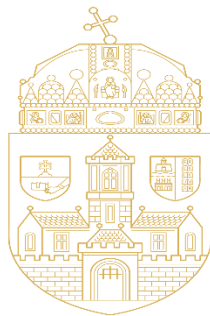
By

Hassanen L. Jaber

M.Sc. in Materials Sciences and Engineering

Supervisor

Dr. Kovács Tünde



ÓBUDAI EGYETEM
ÓBUDA UNIVERSITY

Óbuda University, Doctoral School on Materials Sciences and Technologies

Budapest, Hungary
2022

Introduction

Selective laser melting (SLM) is a type of fusion additive manufacturing technology in which a laser beam is selectively scanned to melt a powder of materials (layer by layer) by an optics and scanner system. Titanium alloys, especially Ti6Al4V (Ti64), are among the most widely used materials in biomedical engineering thanks to their high biocompatibility, high specific strength, and excellent corrosion resistance. In recent years, there has been considerable interest in manufacturing knee, hip, ankle, maxillofacial, and spinal prostheses by SLM based on medical imaging instead of casting and forging. This is due to the fact that SLM technology has the potential to produce functionally graded materials (FGMs), lattice structures (scaffolds), and complex structures (additional degrees of freedom in design).

Applications of SLM Technology of Ti6Al4V

SLM has many applications in the biomedical, automotive, and aerospace fields. Figure 1 shows medical implants such as dental prosthesis, 3-unit dental bridges, and hip stems made with SLM technology. Automotive applications made with SLM technology include oil pump housings, exhaust manifolds, and water pumps for a motor sports car (see Figure 2). Aerospace metal parts made with SLM technology include the flight crew rest compartment bracket, engine housing, and turbine blade, as shown in Figure 3.



Figure 1: Biomedical parts manufactured by SLM technology: (a) and (b) Dental prosthesis, (c) 3-unit dental bridge, and (d) Hip stems.

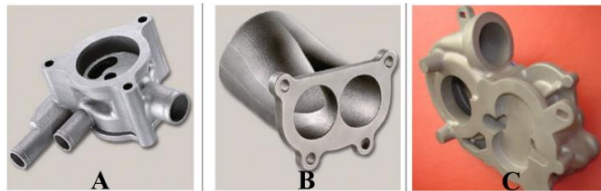


Figure 2: Automotive parts manufactured by SLM technology: (a) Oil pump housing, (b) Exhaust manifold, and (c) Water pump for a motorsport's car.

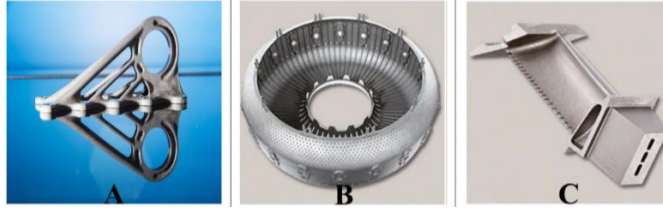


Figure 3: Aerospace parts manufactured by SLM technology: (a) Flight crew rest compartment bracket, (b) Engine housing, and (c) Turbine blade with internal cooling channels.

Outline of the dissertation

The work presented in this dissertation is divided into four chapters.

Chapter 1: Introduction and Motivation

Objectives and research questions

- The first main objective of this chapter was to shed new light on SLM/SLS of Ti alloys and hydroxyapatite to solve a number of the most important problems in metallic implants by using functionally graded materials/structures.
- The second objective of this chapter was to review the current and most important problems of metallic implants that have not yet been solved.
- The third objective of this chapter was to review the effects of SLM parameters on the microstructures and mechanical properties of metallic implants.
- The fourth objective of this chapter was to give a brief overview of the development of Ti alloys.

Chapter 2: Heat Treatments of SLM Ti6Al4V

State of the problem

One of the main issues in the SLM of Ti64 for biomedical implants is the formation of an α' -martensitic microstructure. It has been experimentally demonstrated that SLM parts that are fully α' martensitic have low ductility of less than 10%. Moreover, the residual stresses are associated with the formation of an (α') martensitic structure, resulting in lower mechanical performance. Due to the highly localized heat input, short interaction times, rapid solidification, and large thermal gradients during the SLM process, thermal stresses are formed. In addition, according to

ASTM F13-12a and ASTM F2924-14, the microstructure of an implant or SLM part requires a minimum strain of 10% and an alpha (α)-beta (β) dual phase.

Objective

The purpose of this research is to analyze the effects of annealing and solution treatments at 850 and 1020 °C below and above the β -transus temperature (β_{tr}) on the microstructure and mechanical properties of Ti6Al4V microstructure manufactured by SLM.

Experimental procedure

Four different heat treatments were performed, as shown schematically in Figure 4.

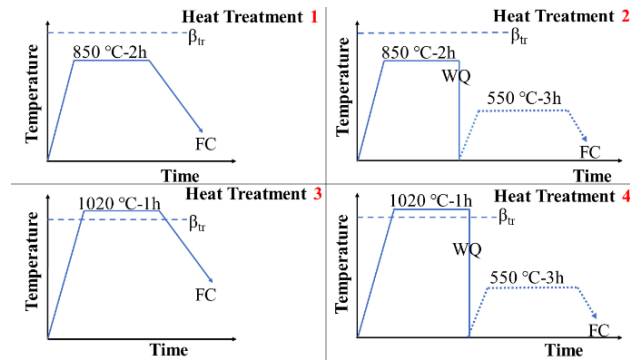


Figure 4: Schematic representation of heat treatment cycle used in this work.

Main Results

Tensile properties

The results of the mechanical properties obtained from the tensile test of as manufactured and heat-treated specimens are summarised and compared in Table 1. As expected, the as-manufactured specimen has a high yield (1060 MPa) and a high ultimate tensile strength (1180 MPa) but a low ductility (8%) of less than 10%. It is important to note that the HT850FC produces the best possible combination of ductility (13%) and strength properties ($\sigma_y=932$, $\sigma_u=986$ MPa) and the microstructure is comprised of β and α phases among all. This is due to the formation of β phase in Ti64 alloy, resulting in a decrease in tensile strength and an increase in ductility.

Table 1: Mechanical properties of the of as printed sample and samples subjected to different heat treatments.

No.	T/°C	t/h	Cooling Rate	Aging			YS/MPa	UTS/MPa	BE%
				T/°C	t/h	Cooling			
1							1060	1180	8
2	850	2	FC	-	-	-	932	986	13
3	850	2	WC	-	-	-	870	930	10.4
4	850	2	WC	550	3	FC	892	970	9.3
5	1020	1	FC	-	-	-	748	833	14.5
6	1020	1	WC	-	-	-	878	990	8.6
7	1020	1	WC	550	3	FC	944	1035	7.2

X-ray diffraction and scanning electron microscopy analysis

Figure 5 reports the XRD pattern of the as-manufactured specimens, in which hexagonal close-packed reflections related to the α' martensite or α phase and a weak orthorhombic reflection related to the α'' martensite of titanium were observed. The SEM experiments (Figure 6) prove that the microstructure of the as-manufactured Ti64 specimens is full α' martensitic, with a lath morphology and a small amount of β phase.

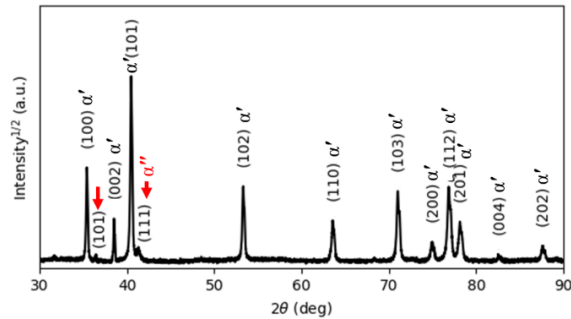


Figure 5: The XRD pattern of the as printed Ti64 indexing α' and α'' phases.

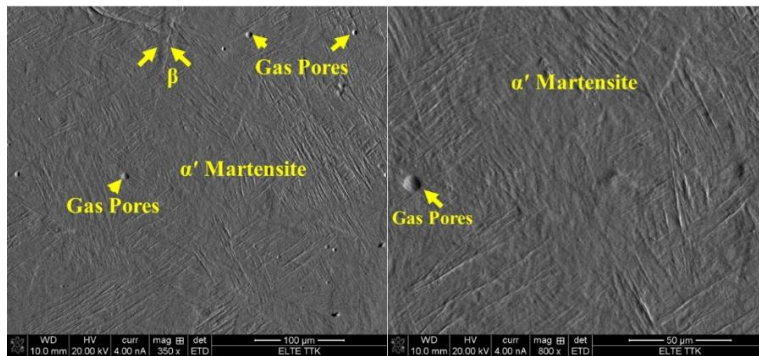


Figure 6: SEM images of Ti64 produced by SLM showing α' martensite microstructure.

Figure 7 reports the X-ray diffraction pattern of the HT850FC specimen in which reflections of the α , β , and α'' phases were observed. The β phase can be seen in the four reflection planes (110), (200), (211), and (220). It is interesting to note that the α'' structure is displayed at a new weak reflection plane of (110) ($2\theta=34.73^\circ$). This would appear to indicate that the α'' is a new phase precipitated from the α' phase during FC cooling. Figure 8 presents the microstructure of the HT850FC specimen at various magnifications, indicating α phase (dark phase) associated with β phase (lighter phase), confirmed by EDS analysis as a V-rich element.

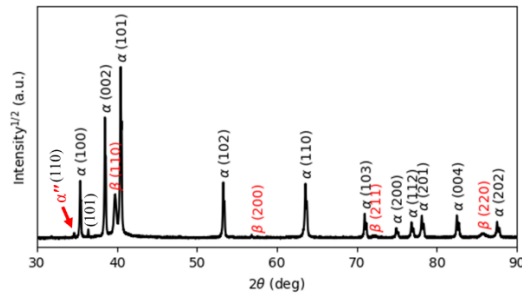


Figure 7: The XRD pattern of the HT850FC sample indexing α , β , and α'' phases.

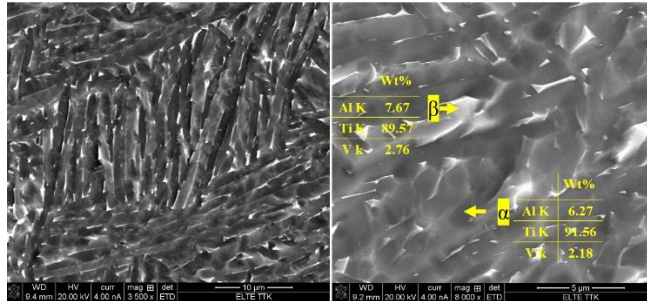


Figure 8: SEM micrographs showing microstructure of the HT850FC sample at different magnifications indicating α phase (dark phase) coupled with β phase (lighter phase).

Chapter 3: Selective Laser Melting of Ti6Al4V-Hydroxyapatite

State of the problem

The resorption of the bone is a process of bone loss resulting from the large difference in Young's modulus between bones (10–30 GPa) and the Ti64 implants (105-110 GPa) for younger patients under 40 years. The significant difference in Young modulus results in a non-gradual transfer of stresses to the bone surrounding the implant, resulting in stress shielding and bone absorption. Stability and fixation of a Ti64 implant inside the bone and bone ingrowth at the interface are the greatest challenges after implantation.

Objective

This work outlines a SLM of Ti64-HA as a composite powder to solve the main Ti64 implant problems. HA was added in order to provide a solid biological fixation between Ti64 implants and bone tissue without the use of bone cements. It is well known that the crystallographic and chemical composition of HA ($\text{Ca}_{10}(\text{PO}_4)_6(\text{OH})_2$) is similar to that of bone tissue, which can dramatically enhance osseointegration and biological fixation.

Experimental procedure

In this work, 2wt% HA powder (nanoXIM•HA203, fluidinova, Portugal) was added into Ti64 powder (Gr.23, LPW Technology/UK) followed by mechanical mixing and SLM processing. Figure 9 shows SEM microscopic images of the mixture of the Ti64 and HA powders and their diameter distributions.

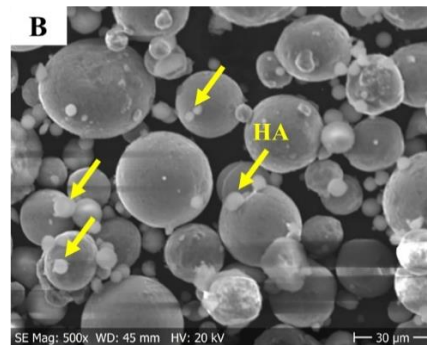


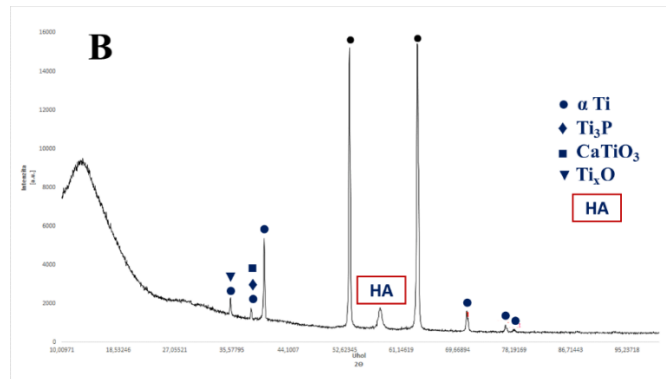
Figure 9: SEM micrograph Ti64 powder mixed with 2 wt% of HA powder.

Main Results

X-ray diffraction and scanning electron microscopy analysis

Figure 10 presents the XRD pattern of the Ti64-2%HA composites in which reflections of α Ti (hcp) and HA phases were revealed. The HA structure is indicated by the peak of $2\theta=57.2^\circ$ which represents the (322) diffraction planes according to (ICDD 00-024-0033). Figure 11 shows typical OM and SEM micrographs of the Ti64-2%HA composite showing the existence of small grain structures associated with dark grain boundaries and some light green areas. Consequently, the microstructure of the SLM of Ti64-2%HA composite is a complex mixture of α Ti, HA, Ti_3P , Ti_xO , P, and CaTiO_3 . The average volume fraction of HA in the microstructure of the Ti64-HA is about 10% based on Image J software. It should be noted that the formation of HA and dispersed

Ca, P, and O elements in the microstructure of implants may result in higher tendency of good bone osseointegration and biocompatibility.



the Ti64-2%HA composite. The higher value of the hardness in the region (563 HV) compared to the vicinity zones (470 HV) can be attributed to the formation of the HA phase.

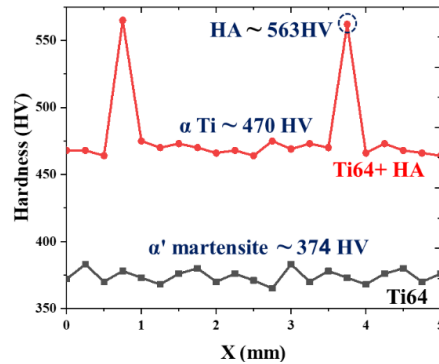


Figure 12: Corresponding microstructures are labelled on Vickers microhardness of the SLM Ti64 and Ti64-2%HA composites.

Chapter 4: SLM Process on Ti6Al4V Alloy Hybrid Powders with Spherical and Irregular Shapes

State of the problem and objective

One of the main obstacles to the use of spherical titanium powder in powder bed additive manufacturing is that it is often expensive (200-450 \$/kg). Irregularly shaped HDH powder is a lower cost product than spherical titanium powder (66-176 \$/kg). For this reason, much attention has been paid to the fabrication of a low-cost hydride-dehydride (HDH) irregularly shaped Ti alloy for powder bed additive manufacturing. Therefore, it is necessary to determine whether the hybrid powder of Ti64 can be printed without affecting the microstructural and mechanical properties of the components fabricated by the SLM system.

Experimental procedure

A hybrid powder (Figure 13) consisting of 50% spherical plasma-atomized (PA) and 50% irregularly shaped hydride-dehydride-based (HDH) Ti64 alloy (provided by TOHO Titanium company/Japan) was used as the starting material. An additional Ti64 (Gr.23) plasma atomized spherical powder (provided by LPW Technology/UK), as demonstrated in Figure 14, was used as a reference powder to facilitate discussion of tensile properties.

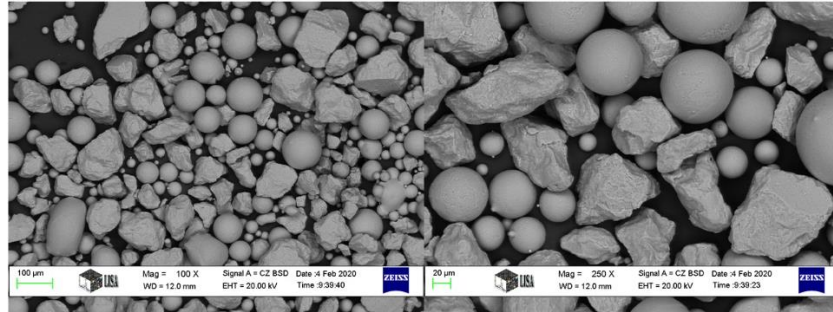


Figure 13: SEM micrograph of Ti64 alloy hybrid powder at two different magnifications.

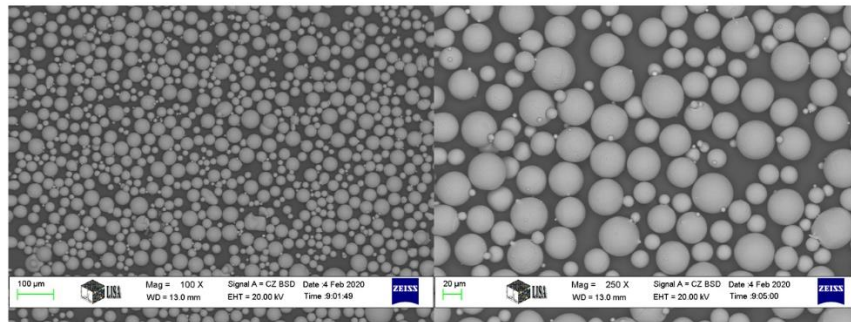


Figure 14: SEM micrograph of Ti64 alloy reference powder at two different magnifications.

Main Results

Formation of defects in building sample

SLM building sample defects made while using hybrid and reference Ti64 powders were determined by examination of the cross-sectional surfaces. Two defects (Figure 15A) were observed during the SEM test in the samples made using the hybrid powder. These included gas porosity, which is accompanied by a spherical or elliptic shape, and lack of fusion voids, which is accompanied by an irregular shape with sharp tips. In contrast, only gas porosity (Figure 15B) was observed in the samples made using the reference powder.

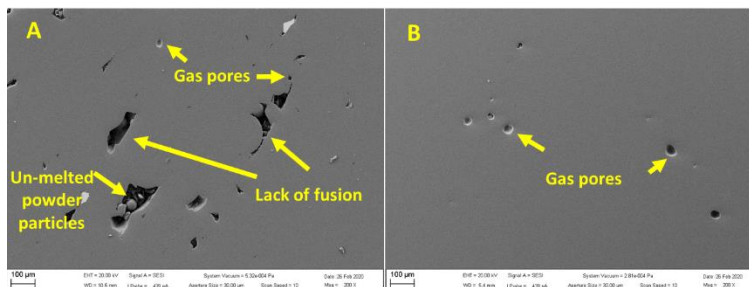


Figure 15: Gas porosity and lack of fusion defects during SLM of A) hybrid powder and B) reference powder.

In contrast with applying 100% spherical powder which leads to high density of fabricated parts, we believe that applying the hybrid powder with its different shape and flowability could leave gaps (or cavities) between such particles which leads to the existence of pores on the final products. In our view, several new techniques can be suggested and will assist researchers in overcoming this problem, including:

- Reducing the hybrid Ti64 powder sizes to a range of 20 to 60 μm ,
- The lack of fusion voids can be reduced by decreasing the amount (ratio) of HDH irregular from 50% to 25% or 15% wt.,
- Using the double scanned or re-melted strategy in order to solve this problem.

Mechanical performance

As highlighted from Figure 16, there is a significant difference in tensile properties between the SLM-fabricated Ti64 parts with 100% spherical powder and SLM-fabricated Ti64 parts with hybrid powder. The average yielding strength, tensile strength, and total elongation of the Ti64 parts manufactured using hybrid powder were 21%, 17%, and 31% lower than that of the Ti64 parts manufactured using 100 wt% spherical powder respectively.

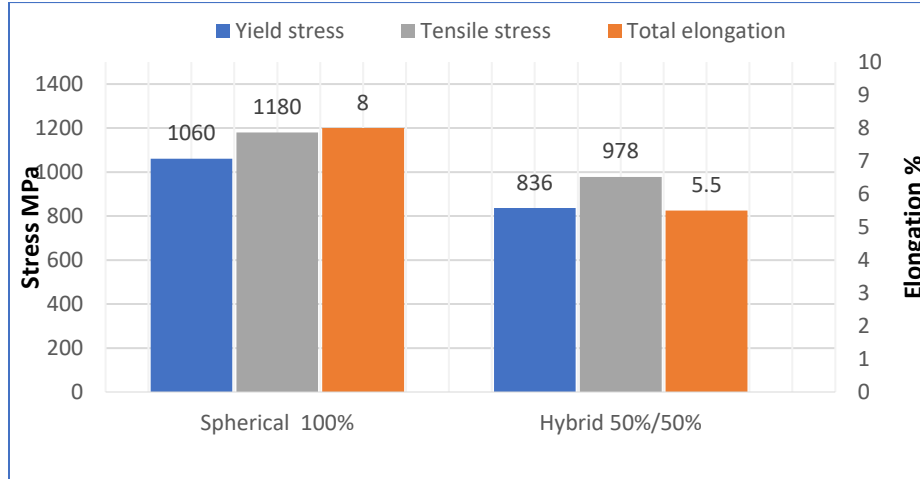


Figure 16: Yielding strength, tensile strength, and total elongation of Ti64 parts manufactured using hybrid powder and spherical powder.

Summary of New Scientific Results

The dissertation findings are summarized in seven thesis points. In square brackets are the author's works in which the actual thesis points were published.

Thesis 1 [Publications: J1]: I have found that the structure of Ti64 manufactured by SLM has two different martensite variants, namely the HCP martensite of the α' -phase and the orthorhombic martensite of the α'' -phase. I also found that the martensitic α' microstructure of as-manufactured Ti64 is characterized by a hierarchical structure composed of four different types of α' based on dimensions: primary ($L = 125 \mu\text{m}$), secondary ($64 \mu\text{m}$), tertiary ($32 \mu\text{m}$), and quaternary ($8 \mu\text{m}$). The parameters of the SLM process were laser power = 125 W, scanning speed = 1000 m/s, and layer thickness = 20 μm .

Thesis 2 [Publications: J1]: I have proved that **solution treatment** at 1020 °C and 850 °C has a slight effect on elongation improvement. After solution treatment at 1020 °C, the elongation increased from 8% (as-printed) to 8.6%, and the tensile strength decreased from 1180 MPa (as-printed) to 990 MPa due to the formation of α , α' , and α'' . After solution treatment at 850 °C, the elongation increased from 8% (as-printed) to 10.4%, and the tensile strength decreased from 1180 MPa (as-printed) to 930 MPa due to the formation of α , β , and α'' .

Thesis 3 [Publications: J1, C1]: I have underlined that the SLM-manufactured Ti64 parts with an **annealing treatment** at 1020 °C followed by cooling in the furnace had higher elongation but significantly reduced strength. The elongation increased from 8% (as-printed) to 14.5 %, and the tensile strength decreased from 1180 MPa (as-printed) to 833 MPa due to the formation of an α and β lamellar structure.

Thesis 4 [Publications: J1]: I have highlighted that **ageing at 550 °C for 3 hours** followed by cooling in the furnace after solution heat treatment at 850 °C and 1020 °C had a negative effect on elongation improvement. After HT850WC + AG (heat treatment at 850 °C followed by water cooling and ageing), the elongation decreased from 10.4% to 9.3%, and the tensile strength increased from 930 MPa to 970 MPa due to the partial dissolution of soft α'' and its transformation into α , β , and α'' . After HT1020WC + AG (heat treatment at 1020 °C followed by water cooling and ageing), the elongation decreased from 8.6% to 7.2%, and the tensile strength increased from 990 MPa to 1035 MPa due to the fragmentation and globalization of longer, elongated α -grains.

Thesis 5 [Publications: J1, C1]: I have demonstrated that the microstructure of HT1020FC (heat treatment at 1020 °C followed by furnace cooling) is characterized by the formation of an $\alpha + \beta$ lamellar structure. In contrast, the microstructure of HT1020WC (heat treatment at 1020 °C followed by water cooling) is characterized by the formation of semi-equiaxial β grains with a diameter of average 170 μm with longer elongated α grains and basket-weave α' . I also demonstrated that the β phase undergoes more complicated microstructural transformations during solidification after HT1020WC, such as the formation of the α' phase by the displacing transformation with a shear mechanism and the formation of the semi-equiaxed β grains morphology by a nucleation process.

Thesis 6 [Publication: J2 and J3]: I have reported the characterization and mechanical properties of a novel Ti6Al4V/2% Hydroxyapatite metal/bio-ceramic composite fabricated using the additive SLM manufacturing process. According to XRD, SEM, EDX (point, line, and maps), OM, and hardness tests, I have revealed that the SLM components made from Ti64-2% HA have small grains of α Ti associated with dark grain boundaries of HA and some light green regions of Ti_3P and other phases of Ti_xO , P and CaTiO_3 . I have showed that the behavior of HA during SLM of Ti64/2%HA goes through two paths: Decomposition and Stability. Part of HA decomposes and interacts with the Ti, which is transformed into Ti_3P , Ti_xO , P, and CaTiO_3 phases. Other HA was stable, and no decomposition occurred. The average volume fraction of HA in the microstructure of Ti64- HA was about 10%.

Thesis 7 [Publication: J3]: I have highlighted that the composite SLM Ti64-2% HA has a heterogeneous hardness profile compared to Ti64, which is due to the formation of different phases in the structure of the composite SLM Ti64-2% HA. The peak microhardness (~ 563 HV) compared to the ambient zones (~ 470 HV) is due to the formation of the phase HA. I have also highlighted that the composite Ti64-2% HA has a higher microhardness (~ 478 HV) than the pure Ti64 (~ 374 HV), which is due to the presence of HA at the grain boundaries and the presence of Ca, P and O elements as a result of the partial decomposition of HA.

List of Publications

Articles in internationally reviewed academic journals

- J1 Hassanen J.**; Kónya, J.; Kulcsár, K.; Kovács, T. Effects of Annealing and Solution Treatments on the Microstructure and Mechanical Properties of Ti6Al4V Manufactured by Selective Laser Melting. *Materials*, 15, 1978, (2022). (WoS, Scopus IF = 4.7, Q1)
<https://doi.org/10.3390/ma15051978>
- J2 Hassanen J.**; Kónya, J.; Anna Kovács, T. Selective Laser Melting of Ti6Al4V-2%Hydroxyapatite Composites: Manufacturing Behavior and Microstructure Evolution. *Metals*, 11, 1295, (2021). (WoS, Scopus IF = 3.8, Q1)
<https://doi.org/10.3390/met11081295>
- J3 Hassanen J.**, Tunde K. Selective laser melting of Ti alloys and hydroxyapatite for tissue engineering: progress and challenges. *Materials Research Express*. Vol 6 No 8:082003. (2019). (WoS, Scopus IF = 4.2, Q1)
<https://doi.org/10.1088/2053-1591/ab1dee>
- J4 Hassanen J.**, Tunde Kovacs & Kónya János. Investigating the impact of a selective laser melting process on Ti6Al4V alloy hybrid powders with spherical and irregular shapes, *Advances in Materials and Processing Technologies*, (2020).
<https://doi.org/10.1080/2374068X.2020.1829960> (WoS, Scopus IF = 3.4, Q2)
- J5 Hassanen J.**, Tunde K. Preparation and Synthesis of Hydroxyapatite Bio-Ceramic from Bovine bone by Thermal Treatment. *Építőanyag: Journal of Silicate Based and Composite Materials*. Vol 71 No 3. Pp. 98-101 (2019). (WoS IF=0.3, Q4)
<https://doi.org/10.14382/epitoanyag-jsbcm.2019.18>

Papers at international scientific conferences

- C1 Hassanen J.**, Tunde K. Development of Selective Laser Melting of Ti6Al4V Alloy for Tissue Engineering: Review. *Bánki Közlemények*. Vol 3 No 1. Pp. 19-23. (2020).
<http://bk.bgk.uni-obuda.hu/index.php/BK/article/view/113/115>
- C2 Hassanen J.**; Kónya, J.; Kulcsár, K.; Kovács, T. The effect of annealing temperature on the microstructure and tensile properties of Ti6Al4V parts produced by selective laser melting. 6TH International Conference on Competitive Materials and Technology Processes, Miskolc. Accepted